World Academy of Science, Engineering and Technology
International Journal of Computer and Information Engineering
Vol:7, No:2, 2013

Texture Feature Extraction of Infrared River Ice Images using Second-Order Spatial Statistics

Bharathi P. T, and P. Subashini

***Abstract*—**Ice cover County has a significant impact on rivers as it affects with the ice melting capacity which results in flooding, restrict navigation, modify the ecosystem and microclimate. River ices are made up of different ice types with varying ice thickness, so surveillance of river ice plays an important role. River ice types are captured using infrared imaging camera which captures the images even during the night times. In this paper the river ice infrared texture images are analysed using first-order statistical methods and second-order statistical methods. The second order statistical methods considered are spatial gray level dependence method, gray level run length method and gray level difference method. The performance of the feature extraction methods are evaluated by using Probabilistic Neural Network classifier and it is found that the first-order statistical method and second-order statistical method yields low accuracy. So the features extracted from the first-order statistical method and second-order statistical method are combined and it is observed that the result of these combined features (First order statistical method + gray level run length method) provides higher accuracy when compared with the features from the first-order statistical method and second-order statistical method alone.

***Keywords*—**Gray Level Difference Method, Gray Level Run Length Method, Kurtosis, Probabilistic Neural Network, Skewness, Spatial Gray Level Dependence Method.

I. Introduction

IMAGE texture, defined as a function of the spatial variation in pixel intensities (gray values), is useful in a variety of image processing applications and has been a subject of passionate study by many researchers. The meaning of the term texture, when image processing is concerned, is completely different from the usual meaning in the field of automated industries. In general, the process of texture analyzing requires the calculation of various features for each texture. Texture features contain information representative of visual characteristics, but also of characteristics which cannot be visually differentiated. The automatic analysis of images requires a first step of digitization which transforms the video signal into a two dimensional matrix of numbers. Each matrix entry is a pixel (picture element) which is the basic components of images with an entire value called ``grey level''. Usually the grey level values are coded with an eight bit numbers, allows in distinguishing of 256 grey levels from 0 (black) to 255 (white). Each pixel will contain two kinds of information. They are brightness value and locations in the coordinates that are assigned to the images. The former is the color feature while features extracted from the latter are known as size or shape features. The texture image analysis is implemented to characterize an object or a texture surface in an image, particular by analysing the texture. Application of image texture is the recognition of image regions using texture properties [19]. Texture study and analysis play a vital role in many image processing applications. "There are four different types of texture, they are statistical texture, structural texture, model based texture and transform based texture. Statistical texture features can be obtained using statistical approaches from the higher order of pixel grey values of images. Structural texture is obtained through some structural primitives constructed from grey values of pixels. Transform based texture can be obtained by using statistical measurements from the images transformed with certain methods. Model based texture can be attained by calculating coefficients from a model based on the relationship of the grey values between a pixel and its neighboring pixels", [24].

Rivers and streams are the key elements in the terrestrial restructuring of water. This is mainly found in winter season, when the overland flow is minimal. Ice cover area has a major impact on rivers as it affects the discharge capacity which results in flooding, restrict navigation, modify the ecosystem and microclimate. Canada is renowned for its magnificent rivers, its harsh but beautiful winters and its large hydroelectricity industry. The impact of the winter regime of Canadian rivers on the operation of hydroelectric facilities extensive monitoring of the river ice cover is necessary [15]. Scientist has reported that "Canada in just six years has lost nearly 50 percent of the massive ice shelf area that holds back glacial ice from melting into the ocean. Two of Canada's biggest ice shelves diminished significantly this summer, one nearly disappearing altogether. The two are among six that make up Canada's biggest shelves, all located on Ellesmere Island. The loss is important as a marker of global warming. Due to global warming winter temperatures have risen by about 1.8 degrees Fahrenheit per decade for the past five to six decades on northern Ellesmere Island", [16].

Application of infrared imaging is used extensively in the field, environmental monitoring, industrial facility inspections, remote temperature sensing, short-ranged wireless communication and spectroscopy, weather fore-casting, military and civilian purposes. Texture feature analysis is the key method that plays an important role in many image processing fields, i.e. segmentation, pattern recognition, classification etc [21, 23]. "Image texture can be evaluated using the properties such as fineness, smoothness, coarseness,

Bharathi P. T, Research Scholar, Department of Computer Science, Avinashilingam Institute of Home Science and Higher Education for Women, Coimbatore, India. (phone: +919952868179; e-mail: bharathi2028@gmail.com).

Dr. P. Subashini, Associate Professor, Department of Computer Science, Avinashilingam Institute of Home Science and Higher Education for Women, Coimbatore, India. (phone: +919442271971; e-mail: mail.p.subashini@gmail.com).

granulation etc. Various statistical and structural methods have been developed to study these features. Statistical methods gained preference over structural methods as most image textures do not follow a specific grammar or rule, which is essential for the successful implementation of structural methods. The statistical methods followed are of different order based on the number of gray values considered for analysis and the type of relationship used. The statistical methods involve calculation of properties based on the gray tones of the specimens. The first-order statistics involves the computation and extraction of features such as mean, variance, standard-deviation, skewness and kurtosis from the histograms of the images. The earliest approach towards higher-order statistics was developed by Haralick et al [1]. They used the co-occurrence matrix approach for the calculation of various features based on the matrices and successfully employed it to the classification of images", [3].

In this paper, the river ice Infrared images are used to study the ice condition of Canadian environment. The ice images are captured with FLIR T640 IR camera. The size of the images are 640 x 480 (307,200 pixels) for greater accuracy and readability from longer range distances. FLIR T640 IR camera captured the image with the temperature ranging from -40°C to +10°C. The infrared texture surfaces are analysed using both the first order statistical method and second order statistical methods. Second order statistical methods are Spatial Gray Level Dependence Method (SGLDM), Gray Level Run Length Method (GLRLM) and Gray Level Difference Method (GLDM). Different textural features are extracted from second order statistical methods. The images used in this paper are given in Fig 1.

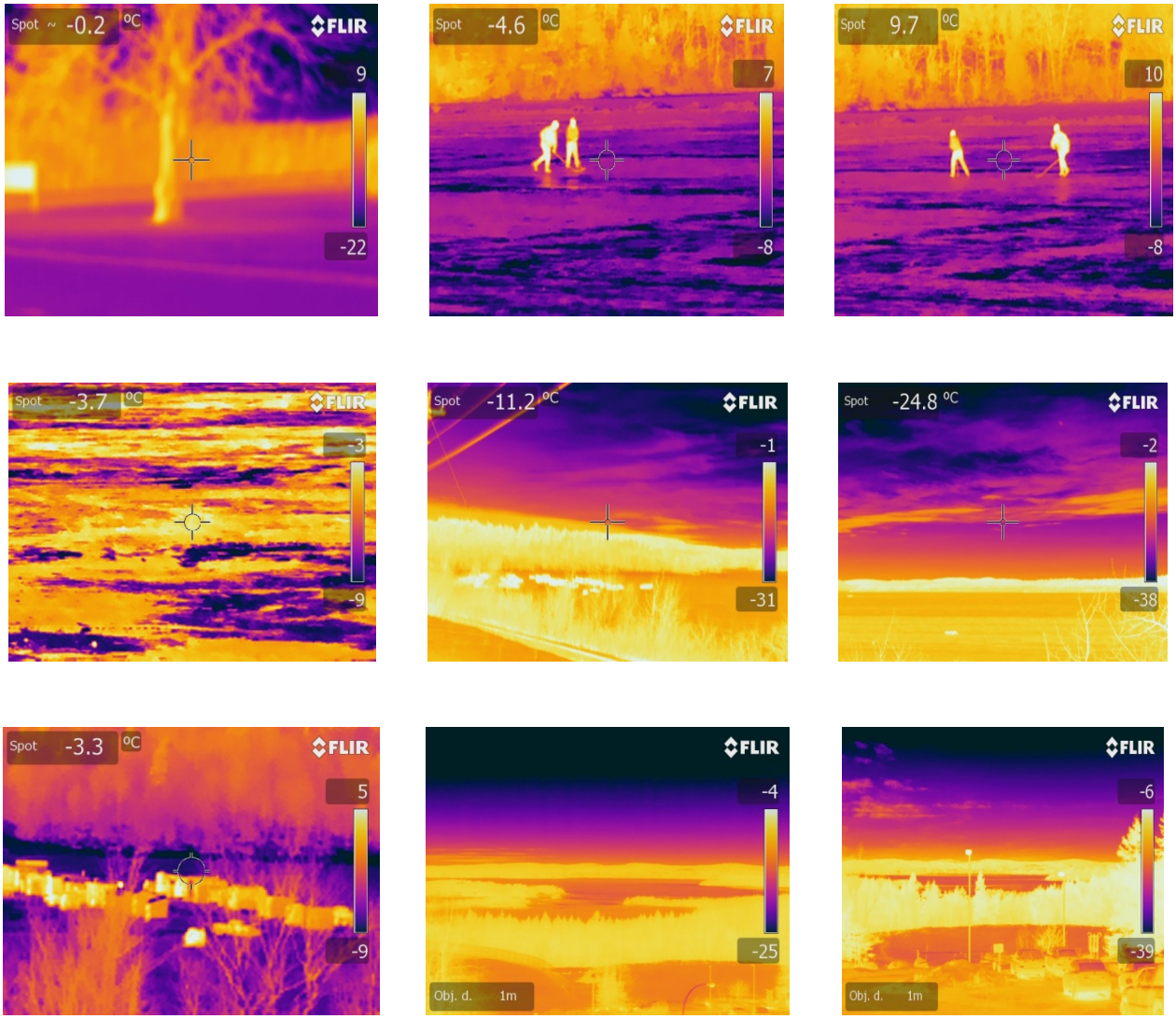

Fig. 1 Infrared ice images (Image 1 to Image 9) with varying temperature range

Flow of the work is structured into four sections. Section 2 introduces about different texture analysis methods. Section 3 presents implementation and experimental results of texture analysis. The conclusions are summarized in Section 4 and

finally all the references been made for completion of this work.

II. Different Texture Analysis Methods

Texture features can be usually classified into four categories as statistical texture, structural texture, model based texture and transform based texture [27]. In texture analysis field, statistical texture is the most widely used method for quality grading or classification [25, 28]. Transform based texture and model based texture might also be used, but not as often as statistical texture. Statistical texture methods include grey level co-occurrence matrix, grey level pixel run length matrix and neighboring grey level dependence matrix while fractal model and auto regression model are model based texture analysis methods. Additionally, convolution mask, Fourier transform and wavelet transform are the most common approaches to obtain transform based texture. Texture analysis methods used in this work are shown in fig 2.

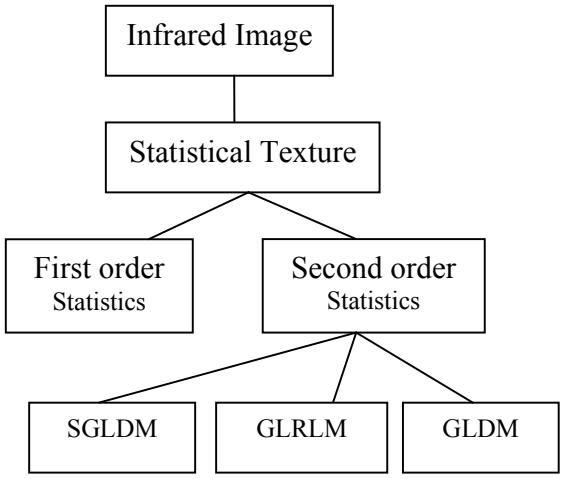

Fig. 2 Texture analysis methods

Statistical texture methods can be classified in two categories. Firstly, the first order statistical methods are characterized by the pixel grey level distribution and organisation. Secondly, the second order statistical methods such as SGLDM, GLRLM and GLDM are considered. Texture image analysis procedure can be defined as a system in which input is an image and the output is a series of features provided by the analysing techniques implemented. Each image is then characterized by a vector of features.

A. First Order Statistical Features

First order statistical feature measures the probability of observing a gray value at a randomly chosen location in the image. First order statistics can be computed from the histogram of pixel intensities in the image. These depend only on individual pixel values and not on the interaction or co-occurrence of neighboring pixel values. The average intensity in an image is an example of the first order statistic [19]. The reason behind this is the fact that the spatial distribution of gray values is one of the defining qualities of texture. First order statistical texture measures are calculated directly from the original image values, like mean, standard deviation, variance, kurtosis and Skewness [16, 17], which do not consider pixel neighborhood relationships [26].

B. Spatial Gray Level Dependency Matrices/ Gray Level Co-Occurrence Matrices

One of the recognized statistical tools for extracting texture information from images is the gray level co-occurrence matrix. Originally introduced by Haralick, et al [1], SGLDM measures second order texture characteristics which play an important role in human vision and has been shown to achieve a similar level of classification performance. This technique is commonly used in texture analysis because it provides for each sample a large set of features and it can be assumed that at least one of these features reflects the small variation of texture between classes. The SGLDM of an $N_x \times N_y$ image, containing pixels with gray levels (0, 1,. . . , G-1) is a two dimensional matrix P(i, j), where each element of the matrix represents the probability of joint occurrence of intensity levels k and l at a certain distance d and an angle θ. The following features were calculated from the co-occurrence matrix for d=1 and four main directions (0°, 45°, 90° and 135°). Before building the matrix, two parameters θ (direction of the pixel pairs) and d (distance between the pixel pairs) as shown in Fig 3 need to be chosen. The SGLDM is obtained by specifying a matrix of relative frequencies P_{ij}, with two neighboring resolution cells separated by distance d occur on the image, one with gray tone i and the other with gray tone j. In general, the matrices P_θ (i, j |d), where θ is the direction of evaluation with distance d. Here d ranges from 1 to d_{max} and i, j are taken over all gray levels [10 – 14, 20]. Generally, rather than using a single displacement one uses a set of displacements to obtain the desired property to which the textural feature corresponds. From the co-occurrence matrix 14 features of texture can then be calculated [1, 2]. However, these 14 features are not independent of each other as some of them might indicate the same image texture properties. Unfortunately, it is still unclear which feature can be ignored.

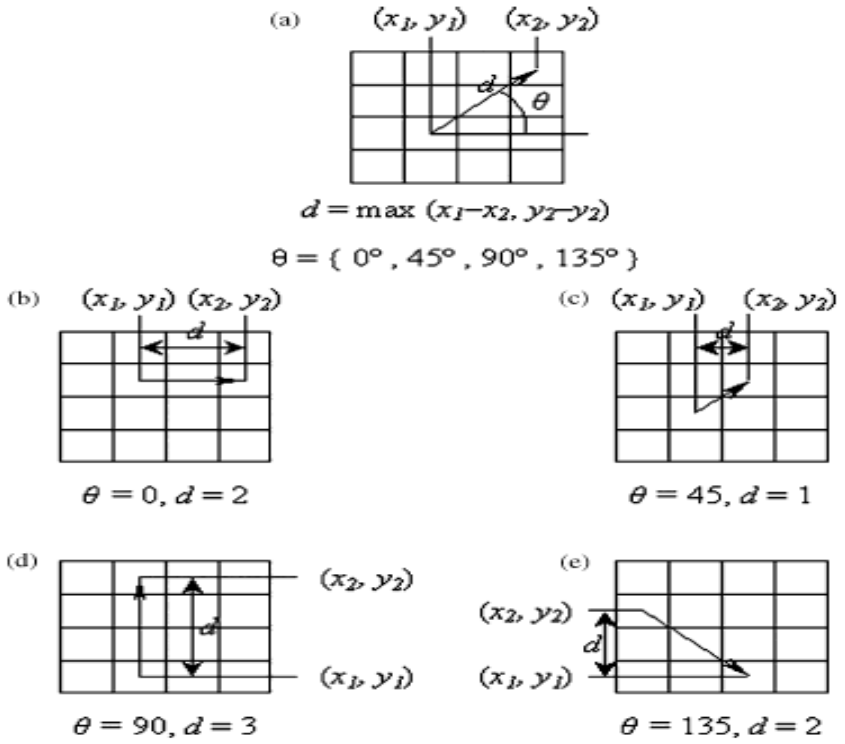

Fig. 3 The direction (θ) of the pixel pairs and the distance (d) between the pixel pairs used to construct the gray level dependency matrix. (a) Illustration of direction (θ) and distance (d) in images of pixel pairs(x_1, y_1) and (x_2, y_2); (b)-(e) are four examples at direction 0, 45, 90, 135^0 respectively

The formulae used for the metrics of the spatial gray level dependency matrix are as follows for the eleven features that are used in this study are as given below:

Contrast (CON):

$$CON = \sum_{n=0}^{N_g-1} n^2 \left\{ \sum_{\substack{i=1 \\ |i-j|=n}}^{N_g} \sum_{j=1}^{N_g} p(i,j) \right\} \quad (1)$$

Correlation (CORR):

$$CORR = \frac{\left[\sum_{i=1}^{N_g} \sum_{j=1}^{N_g} (i,j) p(i,j) \right] - \mu_x \mu_y}{\sigma_x \sigma_y} \quad (2)$$

$$\mu_x = \sum_{i=1}^{N_g} \left[i \sum_{j=1}^{N_g} p(i,j) \right] \qquad \mu_y = \sum_{j=1}^{N_g} \left[j \sum_{i=1}^{N_g} p(i,j) \right]$$

$$\sigma_x = \sum_{i=1}^{N_g} \left[(i - \mu_x)^2 j \sum_{j=1}^{N_g} p(i,j) \right]$$

$$\sigma_y = \sum_{j=1}^{N_g} \left[(j - \mu_y)^2 i \sum_{i=1}^{N_g} p(i,j) \right]$$

Where μ_x , μ_y are the mean values and σ_x , σ_y are the standard deviations of P_x and P_y, respectively

Energy (ENER):

$$ENER = \sum_{i=1}^{N_g} \sum_{j=1}^{N_g} P(i,j)^2 \quad (3)$$

Entropy (ENT):

$$ENT = \sum_{i=1}^{N_g} \sum_{j=1}^{N_g} [P(i,j) \log(P(i,j))] \quad (4)$$

Inverse difference moment (IDM):

$$IDM = \sum_{i=1}^{N_g} \sum_{j=1}^{N_g} \left[\frac{1}{1 + (i-j)^2} P(i,j) \right] \quad (5)$$

Sum of Squares (SOS):

$$SOS = \sum_{i=1}^{N_g} \sum_{j=1}^{N_g} (i - \mu)^2 \, p(i,j) \quad (6)$$

Sum average (SA):

$$SA = \sum_{i=2}^{2N_g} \left[i \; P_{x+y}(i) \right] \tag{7}$$

Sum Variance (SV):

$$SV = \sum_{i=2}^{2N_g} \left[(i - SA)^2 \; P_{x+y}(i) \right] \tag{8}$$

Sum Entropy (SE):

$$SE = -\sum_{i=2}^{2N_g} \left[P_{x+y}(i) \log \left[P_{x+y}(i) \right] \right] \tag{9}$$

Difference Variance (DV):

$$DV = \sum_{i=0}^{N_g - 1} \left[(i - f')^2 \, P_{x-y}(i) \right] \tag{10}$$

Where $$f' = \sum_{i=0}^{N_g - 1} \left[i \, P_{x-y}(i) \right]$$

Difference Entropy (DE):

$$DE = -\sum_{i=2}^{N_g - 1} \left[P_{x-y}(i) \log \left[P_{x-y}(i) \right] \right] \tag{11}$$

C. Gray Level Run Length Method

"Two kinds of methods are used for processing the grey level pixel-run length. In the first one, a vector considering pixel-runs is created from the function q(L, θ, T), in which L is length of the pixel-run (number of pixels in the pixel-run) while θ is direction of the pixel run and T, the threshold. Direction θ of pixel-run is defined similar to that in the GLCM method. Threshold value T for pixels to be merged into the pixel-run is given manually by the user. The procedure of constructing the pixel-runs is as follows: each pixel row of image at direction θ is scanned and the first pixel of the row is set to be the first pixel-run with length 1 and same grey value I as the first pixel; then the next pixel in the row is scanned; if $| I - I_n | \le T$ (I_n is the grey value of the next pixel), the next pixel is merged into the pixel-run, otherwise, a new pixel-run is created and the pointer is moved to the next pixel". This procedure is performed until the scanning of the entire row is completed, and a new row is started [22]. Fig. 4(a) shows an image values and the pixel runs of similar values are build from an original image.

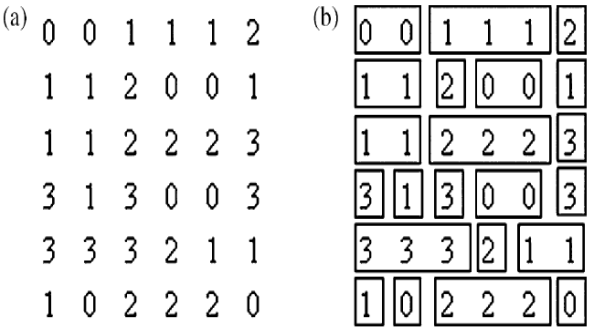

Fig. 4 Illustrations of building the pixel run lengths. (a) Initial input image; (b) Building the pixel run lengths with threshold T = 0 and direction $\theta = 0$

In the GLRLM approach, the gray level runs are characterized by the gray tone of the run and the length of the run and the direction of the run [18]. "Let P(i, j) represent the run length matrix array. The matrix array consists of elements with the gray tone "i" has a run length "j". Textural features are calculated from the array elements that are used to study the nature of image textures. From the original run length matrix p(i, j), many numerical texture measures can be computed. The five original features of run length statistics derived by Galloway", [5] are as follows.

Short Run Emphasis (SRE):

$$SRE = \frac{1}{n_r} \sum_{j=1}^{N} \frac{P_r(j)}{j^2} \tag{12}$$

Long Run Emphasis (LRE):

$$LRE = \frac{1}{n_r} \sum_{j=1}^{N} P_r(j) \cdot j^2 \tag{13}$$

Gray-Level Nonuniformity (GLN):

$$GLN = \frac{1}{n_r} \sum_{i=1}^{M} P_g(i)^2 \tag{14}$$

Run Percentage (RP):

$$RP = \frac{n_r}{n_p} \tag{15}$$

Run Length Nonuniformity (RLN):

$$RLN = \frac{1}{n_r}\sum_{j=1}^{N} P_r(i)^2 \quad (16)$$

Low Gray-Level Run Emphasis (LGRE):

$$LGRE = \frac{1}{n_r}\sum_{i=1}^{M} \frac{P_g(i)}{i^2} \quad (17)$$

High Gray-Level Run Emphasis (HGRE):

$$HGRE = \frac{1}{n_r}\sum_{i=1}^{M} P_g(i).i^2 \quad (18)$$

"In the above equations, n_r is the total number of runs and n_p is the number of pixels in the image. Based on the observation that most features are only functions of $p_r(j)$, without considering the gray level information contained in $p_g(i)$", Chu et al. [9] proposed two new features, as follows, to extract gray level information in the matrix.

D.Gray Level Difference Method

The run difference method is a generalized form of the GLDM, which is based on the estimation of the pdf of gray level differences in an image. GLDM seeks to extract texture features that describe the size and prominence of textural elements in an image. "Let I(x, y) be the image intensity function. For any given displacement δ = (ΔX , ΔY) let I δ (x, y) = |I(x, y) - I(X + ΔX , Y + ΔY)|, and f(i| δ) be the probability density of I δ (x, y). The value of f(i| δ) is obtained from the number of times I δ (x, y) occurs for a given δ, i.e. f(i| δ) = P(I δ (x, y) = i). If a texture is directional, the degree of spread of the values in f(i| δ) should vary with the direction of d, given that its magnitude is in the proper range. Thus, texture directionality can be analyzed by comparing spread measures of f(i| δ) for various directions of d. In the present study, four possible forms of the vector d were considered: (0, d), (d, 0), (-d, d), and (-d, -d), with d being the inter pixel distance, each of which corresponds to a displacement in 0^0, 45^0, 90^0 and 135^0 direction, respectively. From each of the density functions corresponding to one of the above-mentioned directions, five texture features were obtained" [6, 7, 8]:

$$I_{rgdif} = \sum_{\theta \in \Theta} I^{\theta}_{rgdif} \quad (19)$$

From which statistical measures are extracted from the distribution of gray level differences. Rather than extracting textural features directly from the matrix I, three characteristic vectors are calculated to define texture descriptors.

The distribution of gray level differences (DGD) vector is computed as follows:

$$DGD_j = \sum_{r=1}^{[S/2]} I_{grdif} \quad (20)$$

The distribution of the average gray level difference given r is represented by the DOD vector

$$DOD_r = \sum_{gdif=0}^{G-1} g_{dif} I_{rgdif} \quad (21)$$

and the distribution of the average distance given g_{dif} is represented by the DAD vector

$$DAD_j = \sum_{r=1}^{[S/2]} rI_{rgdif} \quad (22)$$

Five features that describe the distribution of gray level differences are defined from these characteristic vectors:

Large difference emphasis (LDE), which measures the predominance of large gray level differences;

$$LDE = \sum_{j=0}^{n_g} DGD(j).\ln\left(\frac{K}{j}\right) \quad (23)$$

Where K is a constant

Sharpness (SHP), which measures the contrast and definition in an image;

$$SHP = \sum_{j=0}^{n_g} DGD(j).j^2 \quad (24)$$

SMG (Second Moment of DGD), which measures the variation of gray level differences;

$$SMG = \sum_{j=0}^{n_g} DGD(j)^2 \quad (25)$$

SMO (Second Moment of DOD), which measures the variation of average gray level differences;

$$SMO = \sum_{r=1}^{f_{\max}} DOD(r)^2 \quad (26)$$

LDEL (long distance emphasis for large difference), which measures the prominence of large differences a long distance from each other.

$$LDEL = \sum_{j=0}^{n_g} DAD(j).\, j^2 \quad (27)$$

By experiments, three characteristic vectors, DGD, DOD and DAD, are enough to represent a run difference method [31]. The texture features computed from the gray level difference matrices are given in Table IV.

III. Implementation and Experimental Results

Texture feature information is examined by extracting first order statistical values, second order statistical methods such as SGLDM, GLRLM and GLDM. The extracted texture features are evaluated using PNN classifier.

First order statistics of the gray level allocation for each image matrix I(x,y) were examined through five commonly used metrics, namely, mean, variance, standard deviation, skewness and kurtosis as descriptive measurements of the overall gray level distribution of an image. The results of first order statistical method of an infrared river ice image are shown in Table I. The 3D (three dimensional) plots of the SGLDM of the infrared images are shown in Fig 5.

TABLE I
First Order Statistics of the River Ice Infrared Images

Image	Mean	Variance	Standard Deviation	Skew ness	Kurtosis
Img1	109.399	105.826	10.287	0.276	2.181
Img2	93.574	82.296	9.072	0.602	2.451
Img3	104.321	86.329	9.291	0.442	2.303
Img4	137.838	133.399	11.550	-0.451	2.137
Img5	134.333	127.186	11.278	-0.174	1.510
Img6	115.674	106.366	10.313	0.164	1.664
Img7	103.813	102.701	10.134	0.394	3.202
Img8	118.794	133.520	11.555	-0.210	1.486
Img9	132.366	124.795	11.171	-0.275	1.740

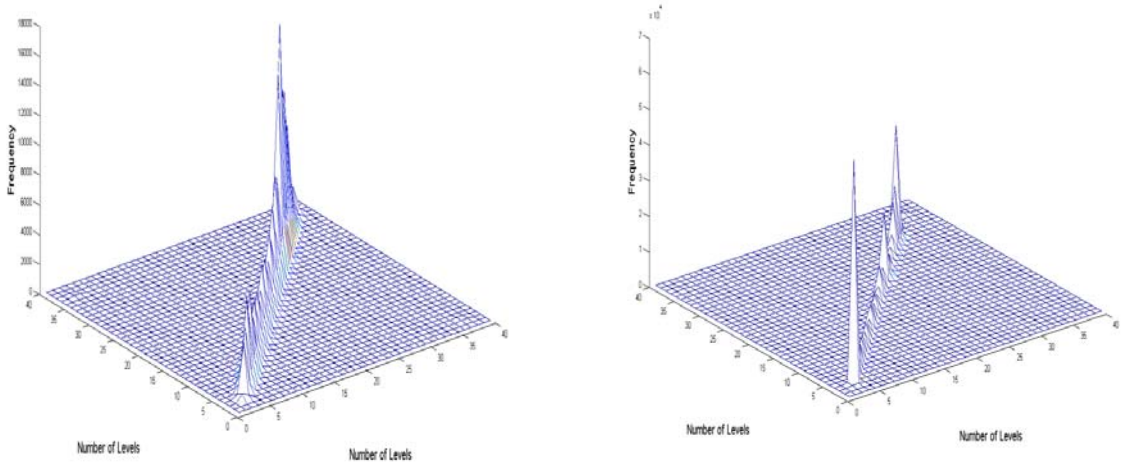

Fig. 5 3-D plots of the spatial gray level dependency matrices of the images

Second order statistics of gray level distribution is derived from SGLDM, are examined through 11 commonly used metrics proposed by Haralick et al.[1]. The co-occurrence matrices are symmetrical, showing the accuracy of calculations. The parameters calculated from the co-occurrence matrices are given in Table II.

In this table, the conventions used are as follows: CON: Contrast, CORR: Correlation, ENER: Energy, ENT: Entropy, IDM: Inverse Difference Moment, "SOS: Sum of Squares, SA: Sum Average, SE: Sum Entropy, SV: Sum Variance, DE: Difference Entropy, DV: Difference Variance. The following observations are made from the plots of these surfaces. In the 3-D plots of the co-occurrence matrices shown, the height of the element is proportional to the matrix element at the corresponding location. The elements of the co-occurrence matrices tend to shift along the diagonal, with the smoother surfaces taking the far end of the principal diagonal. These matrices are found to be more sensitive to changes in surface finish than those calculated from the first order statistics", [3].

TABLE II
TEXTURAL FEATURES CALCULATED FROM THE SPATIAL GRAY LEVEL DEPENDENCY MATRICES

IMAGE	CON	CORR	ENER	ENT	IDM	SOS	SA	SV	SE	DV	DE
Image1	1.077	0.676	0.109	2.703	0.985	18.092	8.081	41.275	2.105	1.077	1.005
Image2	0.906	0.765	0.104	2.653	0.987	14.966	7.113	31.429	2.138	0.906	0.966
Image3	1.044	0.729	0.079	2.828	0.985	17.127	7.701	36.609	2.218	1.044	1.036
Image4	3.314	0.358	0.048	3.390	0.956	25.489	9.601	60.295	2.301	3.314	1.499
Image5	1.117	0.855	0.096	2.748	0.985	25.485	9.488	66.127	2.268	1.117	0.997
Image6	1.021	0.831	0.090	2.797	0.986	19.230	8.300	46.744	2.296	1.021	0.973
Image7	1.910	0.325	0.077	2.951	0.974	16.226	7.694	35.584	2.051	1.910	1.249
Image8	0.981	0.859	0.109	2.674	0.987	21.790	8.728	55.398	2.191	0.981	0.691
Image9	1.265	0.820	0.087	2.826	0.983	24.961	9.433	63.804	2.272	1.265	1.063

Gray level runs are derived from GLRLM method and are examined with the introduction of commonly used run length metrics, proposed by Galloway [5]. Namely, short runs emphasis, long runs emphasis, gray level non-uniformity, run percentage, run-length non-uniformity, low gray level emphasis and high gray level emphasis were used as descriptive measurements of each of the run-length matrix calculated over the sampled images [4]. The 3 D plots of the GLRLM method is shown in Fig. 6. The texture features computed from the run length matrices are given in Table III and the texture features computed from the GLDM method is shown in Table IV.

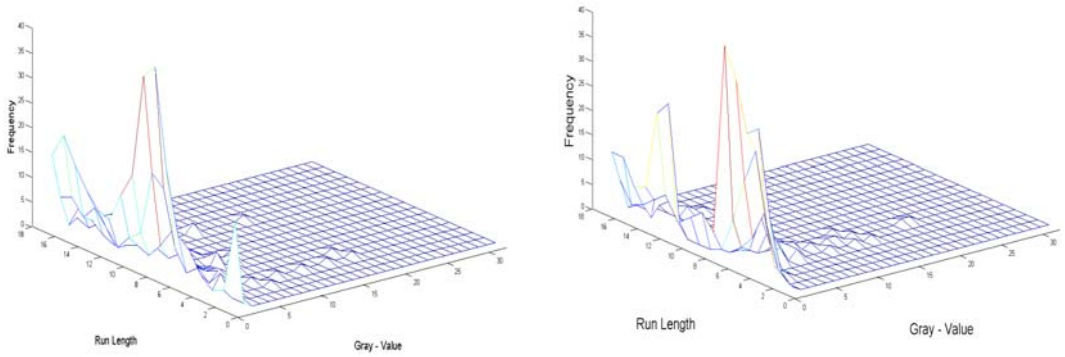

Fig. 6 3-D plots of the gray level run length matrices of the images

TABLE III
GRAY LEVEL RUN-LENGTH PARAMETERS OF THE MATRICES

IMAGE	SRE	LRE	GLN	RP	RLN	LGRE	HGRE
Image1	0.459	418.331	205.371	0.132	458.765	0.023	131.837
Image2	0.471	132.985	469.980	0.187	663.867	0.034	140.254
Image3	0.497	96.811	544.379	0.214	826.561	0.037	126.037
Image4	0.400	56.589	399.583	0.227	654.782	0.016	157.547
Image5	0.516	75.501	265.032	0.246	1044.939	0.043	99.219
Image6	0.449	720.702	191.846	0.084	262.029	0.240	47.621
Image7	0.509	174.637	307.245	0.158	626.521	0.030	97.126
Image8	0.504	2086.906	57.839	0.047	199.114	0.178	80.425
Image9	0.264	354.254	127.773	0.114	187.738	0.098	84.858

TABLE IV
GRAY LEVEL DIFFERENCE MATRIX PARAMETERS

IMAGES	*LDE*	*SHP*	*SMG*	*SMO*	*LDEL*
Image1	1.4896E+01	6.1793E+02	2.3158E+03	4.1133E+02	1.3013E+04
Image2	2.1945E+01	5.1351E+02	2.6800E+03	3.5248E+02	9.8017E+03
Image3	2.3248E+01	4.9999E+02	2.6576E+03	3.6568E+02	9.8033E+03
Image4	2.9020E+00	1.9384E+03	1.6609E+03	7.0678E+02	2.5381E+04
Image5	1.3124E+01	9.7752E+02	2.1499E+03	4.9550E+02	1.8581E+04
Image6	1.7790E+01	6.3089E+02	2.3229E+03	4.2621E+02	1.3185E+04
Image7	1.1704E+01	1.1090E+03	1.9998E+03	5.2952E+02	1.7280E+04
Image8	6.6240E+00	1.2866E+03	1.9140E+03	5.6643E+02	2.2876E+04
Image9	8.0290E+00	1.1164E+03	1.9290E+03	5.5061E+02	2.0647E+04

A. PNN Classifier

"Probabilistic Neural Networks (PNN) is a widely used in classification methodology, because of its simplicity, robustness to noise, fast training speed, fast online speed, no local minima issues and training samples can be added or removed without extensive retraining. PNNs main task is the classification of unknown feature vectors into predefined classes, where the Probability Density Function (PDF) of each class is estimated by kernel functions", [29, 30]. On receiving a pattern X from the input layer, the neuron X_{ij} of the pattern layer computes its output. The output of pattern layer is represented by

$$Y_{ij}(X)=e^{-|X-X_{ij}|2}/\sigma^2 \qquad i,j=1,2,...n \tag{28}$$

Where 'n' represents number of training sets, σ is the smoothing parameter. The summation layer neurons compute the pattern X being classified.

B. Performance Rate

"The performance rate is a useful tool to assess the prediction performance of the models. A correct prediction is counted when the predicted value is consistent with the observed. The performance rates of PNN model were computed on calibration and validation data sets using equation", [29]. The results of the PNNs classifier are shown in Table V. It is observed that the PNN classifier provides 84% accuracy for the combination of First order statistical method and GLRLM method for infrared river ice images.

$$Performanæ\ rate(\%) = 100 * \frac{Number\ of\ correct\ prediction}{Number\ of\ data} \tag{29}$$

The texture features which are extracted by using first order statistical method, second order statistical methods such as SGLDM, GLRLM, and GLDM give less accuracy rate. So in order to improve the accuracy rate of classification the two feature extraction methods are combined to form a feature set. The new feature set is evaluated using PNN classifier. It is observed that the new feature set (First order statistics + GLRLM) improves the accuracy rate when compared with other feature extraction methods. The results of all the above mentioned methods are shown in table V and the classification accuracy graph is shown in fig 7.

TABLE V
PNN CLASSIFIER ACCURACY FOR THE FEATURE EXTRACTION METHODS

FEATURE EXTRACTION METHODS	*CLASSIFIED*	*MISCLASSIFIED*	*ACCURACY IN (%)*	*ERROR RATE*
First Order	12	6	67	33
SGLDM	12	6	67	33
GLRLM	11	7	61	39
GLDM	7	11	38	62
First Order + SGLDM	12	6	67	33
First Order + GLRLM	15	3	84	26

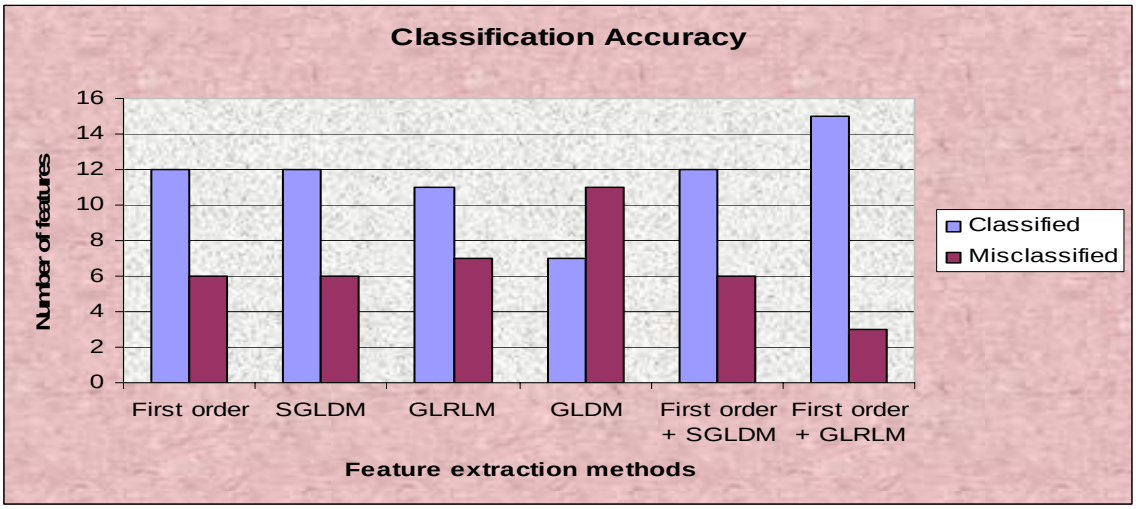

Fig. 7 PNN Classification accuracy

IV. Conclusion

In this experimental work, the region which is covered with river ice affects in flooding, restrict navigation. In order to prevent the affects from river ice and caution the people around the ice covered region, the images are captured using infrared camera. The images contain different textures, so the texture surfaces are analysed using first-order statistics and second-order statistics. The techniques for the second order statistics that have been examined are the spatial gray level dependence method, gray level run length method and gray level difference method. The performance of the feature extraction methods are evaluated by using PNN classifier and it is found that the first and second order statistics yields low accuracy. In order to improve the accuracy level the first and second order methods are combined, by which the accuracy rate is improved when compared with only first and second order methods. The combined features (First order statistical + GLRLM) when used for texture classification of river ice infrared texture surfaces gives better accuracy.

References

[1] Robert M Haralick et al, "Textural features for Image classification", IEEE Transactions on systems, Man and cybernetics, Vol. Smc – 3, No. 6, November 1973, pp 610 – 621.

[2] Hall – Beyer. M, "The GLCM Texture tutorial", version 2.8 (www.fp.ucalgary.ca/mhallbey/the-glcm.htm, university of Calgary, Canada).

[3] K. Venkat Ramana and B. Ramamoorthy, "Statistical Methods to Compare the Texture Features of Machined Surfaces", *Pattern Recognition*, Vol. 29, No. 9, pp. 1447 1459, 1996.

[4] Michael E. Mavroforakis et al, "Mammographic masses characterization based on localized texture and dataset fractal analysis using linear, neural and support vector machine classifiers", Artificial Intelligence in Medicine (2006) 37, 145—162.

[5] Galloway M, "Texture analysis using gray level run lengths", Comp Graph Im Proc 1975; 4:172-9.

[6] Shoshana Rosskamm, "Computer Aided Diagnosis of Cystic Fibrosis and Pulmonary Sarcoidosis using Texture Descriptors Extracted from CT Images", thesis for the Master of Science degree of Applied Mathematics 2010.

[7] Stavroula G. Mougiakakou et al, "Differential diagnosis of CT focal liver lesions using texture features, feature selection and ensemble driven classifiers", Elsevier Artificial Intelligence in Medicine (2007) 41, 25—37.

[8] Wei-Ming Chen et al., "3-D Ultrasound Texture Classification using Run Difference Matrix", Elsevier Ultrasound in Med. & Biol., Vol. 31, No. 6, pp. 763–770, 2005.

[9] Chu, C. M. Sehgal, and J. F. Greenleaf, "Use of gray value distribution of run lengths for texture analysis", Pattern Recognit. Lett, Vol. 11, pp. 415–420. June 1990.

[10] Fritz Albregtsen, "Statistical Texture Measures Computed from Gray Level Coocurrence Matrices", Image Processing Laboratory Department of Informatics University of Oslo, November 5, 2008.

[11] M. M. Mokji, "Gray Level Co-Occurrence Matrix Computation Based on Haar Wavelet", IEEE Trans, Computer Graphics, Imaging and Visualisation CGIV 2007.

[12] E. R. Davies, "Introduction to Texture Analysis", Handbook of Texture Analysis © Imperial College Press.

[13] Foucherot et al., "New methods for analysing colour texture based on the Karhunen–Loeve transform and quantification", Pattern Recognition Society. Published by Elsevier Ltd, 2004.

[14] D. Chappard et al., "Image analysis measurements of roughness by texture and fractal analysis correlate with contact profilometry", Elsevier, Biomaterials 24, 2003, page no. 1399–1407.

[15] Yves Gauthier et al., "A combined classification scheme to characterize river ice from SAR data", EARSel eProceedings 5, 1/2006.

[16] Bharathi .P. T and P. Subashini, "De-noising filters for impulse noise in Glacier ice Infrared images", International Conference on Advances in image Processing and Computation Techniques (PCT) 2012.

[17] Bharathi P.T and P. Subashini, "Automatic identification of noise in ice images using statistical features", Fourth International Conference on Digital Image Processing (ICDIP), April 2012.

[18] Xiaoou Tang, "Texture Information in Run-Length Matrices", IEEE Transactions On Image Processing, Vol. 7, No. 11, November 1998.

[19] Mihran Tuceryan and Anil K. Jain, "Texture Analysis", The Handbook of Pattern Recognition and Computer Vision (2nd Edition), by C. H. Chen, L. F. Pau, P. S. P. Wang (eds.), pp. 207-248, World Scientific Publishing Co., 1998.

[20] G.R.J. Cooper et al., "The use of textural analysis to locate features in geophysical data", Elsevier Computers & Geosciences 31 2005, page no. 882–890.

[21] Christopher Spain, "Automatic Detection of Explosive Devices in Infrared Imagery using Texture with Adaptive Background Mixture Models", Master Of Science Thesis, May 2011.

[22] F. R. Renzetti, L. Zortea, "Use of a gray level co-occurrence matrix to characterize duplex stainless steel phases microstructure", *Fratturaed Integrità Strutturale, 16 (2011) 43-51.*

[23] Graziano Aretusi et al., "Texture Analysis in Thermal Infrared Imaging for Classification ff Raynaud's Phenomenon".

[24] Chaoxin Zheng et al., "Recent applications of image texture for evaluation of food qualities—a review", Elsevier Trends in Food Science & Technology 17 (2006) 113–128.

[25] Patel, D., Hannah, I., & Davies, E. R, "Foreign object detection via texture analysis", 12th IAPR international conference on pattern recognition Proceeding: Vol. 1. Conference A: Computer vision and image processing, 1994.
[26] Li, J., Tan, J., & Shatadal, P, "Classification of tough and tender beef by image texture analysis", Meat Science, 57, 341–346, 2001.
[27] Bharati M. H, Liu J. J & MacGregor J. F, "Image texture analysis: methods and comparisons", Chemometrics and Intelligence Laboratory Systems, 72, 57–71, 2004.
[28] G. N. Srinivasan, and Shobha G, "Statistical Texture Analysis", Proceedings of World Academy of Science, Engineering and Technology Volume 36 December 2008 ISSN 2070-3740.
[29] Ojala, T. and M Pietikäinen, "Texture Classification", Machine Vision and Media Processing Unit, University of Oulu, Finland.
[30] D. H. TRAN et al, "Application of probabilistic neural networks in modelling structural deterioration of stormwater pipes", Urban Water Journal, Vol. 3, No. 3, September 2006, 175 – 184.
[31] Padma and Dr.R.Sukanesh, "A Wavelet Based Automatic Segmentation of Brain Tumor in CT Images Using Optimal Statistical Texture Features", International Journal of Image Processing (IJIP), Volume (5) : Issue (5) : 2011.